Chiang Mai J. Sci. 2018; 45(5) : 2201-2210
http://epg.science.cmu.ac.th/ejournal/
Contributed Paper

Molecular Aggregation of Four Modified Xyloglucan Models in Aqueous Solution

Napat Kongtaworn [a], Namon Hirun [b], Vimon Tantishaiyakul [c], Thanyada Rungrotmongkol [d,e] and Supaporn Dokmaisrijan* [a]

[a] School of Science, Walailak University, Nakhon Si Thammarat 80161, Thailand.
[b] School of Pharmacy, Walailak University, Nakhon Si Thammarat 80161, Thailand.
[c] Department of Pharmaceutical Chemistry, Faculty of Pharmaceutical Sciences, Prince of Songkla University, Songkhla 90112, Thailand.
[d] Structural and Computational Biology Research Group, Department of Biochemistry, Faculty of Science, Chulalongkorn University, Bangkok 10330, Thailand
[e] Ph.D. Program in Bioinformatics and Computational Biology, Faculty of Science, Chulalongkorn University, Bangkok 10330, Thailand.
* Author for correspondence; e-mail: sdokmaisrijan@yahoo.com

Received: 1 November 2017
Accepted: 30 April 2018

ABSTRACT

Tamarind seed xyloglucan (TSX) is extracted from tamarind seeds and is one of the most useful natural polymers. It has been used as a drug carrier in drug delivery because of its non-toxicity, biodegradability, and biocompatibility. A solution of TSX can become a thermally reversible TSX hydrogel when its galactose molecules are partially removed. It was found that a galactose-removed TSX hydrogel is formed when two modified TSX chains form parallel-like structure in aqueous solution. Many molecular associations via hydrogen bonds between two modified TSX chains can promote its molecular aggregation. Moreover, it was reported that the lack of galactose molecules might be able to promote the aggregation of the β-glucan main chains through the hydrophobic interactions, resulting in the gelation. In this study, four double-chain TSX models with 50% galactose removal were used for the study of molecular aggregation in aqueous solution at its gelling temperature. Each model was built from eight monomer units of nonasaccharide (N, XLLG) and eight monomer units of heptasaccharide (H, XXXG), where G, X, and L are glucose (Glu), xylose (Xyl) substituted with glucose, and galactose (Gal) substituted with xyloglucose, respectively. The numbers of N and H are equal in all models, but the arrangements of N and H monomer units in each model are different. The simulated SAXS profiles of all models were also carried out. The roles of molecular structures, intermolecular interactions, and molecular arrangements in molecular aggregation of 50% galactose removal of two TSX chains are discussed.

Keywords: tamarind seed xyloglucan, hydrogel, SAXS, MD simulation

1. INTRODUCTION

Tamarind seed xyloglucan (TSX) is a hemicellulose polysaccharide that has been widely used in drug delivery [1-9]. It is extracted from the seed of *Tamarindus indica* [10-13] and it is a non-toxic, biocompatible and biodegradable material. The structure of TSX polymer was reported that it is built from three types of monomer units with the different number of β-D-galactose (Gal) residues (Figure 1). Three monomer units are heptasaccharide (H, XXXG), octasaccharide (O1, XXLG and O2, XLXG), and nonasaccharide (N, XLLG), where G, X, and L are β-D-glucose (Glu), α-D-xylose (Xyl) substituted with β-D-glucose, and β-D-galactose (Gal) substituted with α-D-xyloglucose, respectively [10, 14-16]. The XLLG or N unit was reported to be the most abundant unit of TSX [10, 14-17].

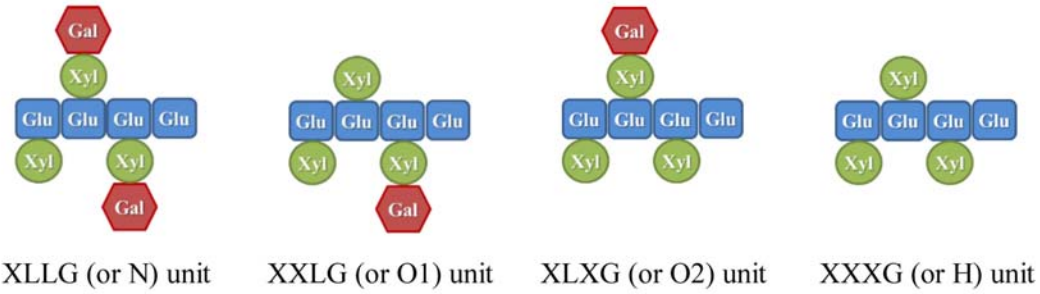

Figure 1. The monomer units of TSX.

The study of the TSX structure, sol-gel transition, and structural behavior of TSX becomes attractive since the structural properties of TSX in the sol and gel states are important for the rationale design of drug vehicles. Many experiments [10, 13, 18-23] such as atomic force microscopy [23] and Small Angle X-ray Scattering (SAXS) [10], have been applied to characterize the nanostructure of the TSX in aqueous solution. The SAXS profiles of TSX monomer units indicated that the H and O1, O2 monomer units could aggregate while the N unit could not aggregate [10]. The aggregation of TSX was observed when Gal was removed and the Gal residue was more hydrophilic than Glu and Xyl residues [24]. Furthermore, the monomer units could have flat conformation and a very dilute solution of native TSX had a rod-like structure [21-22, 25-26]. However, the molecular structures of native TSX and galactose-removed TSX structures have not been reported.

The gelation of TSX has been of great interest in biomaterial science because TSX hydrogel is a temperature-responsive gel [2, 6, 23, 27-33]. It is well-known that natural TSX is water-soluble and cannot form a gel by itself. For the preparation of TSX hydrogel to be used as a drug vehicle, a fungal β-galactosidase is used to partially remove the Gal residue from natural TSX [27, 34-36]. The galactose removal ratio is defined as the percentage of removed Gal from the total number of Gal of native TSX [2, 27, 35]. Moreover, the sol-gel transition temperature decreases when the galactose removal ratio increases [2, 27, 35]. It was reported that the gelation temperature of this galactose-removed TSX is 283 K - 310 K if the Gal removal ratio is ~50% [17, 27, 37].

In this study, the possible structures of 50% galactose removal of two TSX chains in aqueous solution at 283 K and 1 atm were designed and simulated using a molecular dynamics (MD) simulation technique. The most possible structures of the modified TSX model could give the information regarding the types and positions of monomer units of TSX and their intermolecular interactions between two modified TSX chains. Besides, the roles of Gal and Xyl in the clustering of TSX chains could be used to explain the aggregation of TSX polymer and help us understand the gelation behavior and molecular structure of TSX hydrogel.

2. MATERIALS AND METHODS

The molecular structure of a native TSX polymer was believed that it consisted of a large number of XLLG monomer units (or N unit). Nowadays, the molecular structure of any galactose removal TSX structure in the sol and aqueous states has not been reported. In this work, 50% galactose removal of two TSX chains were assigned and constructed by the N and H monomer units. Four initial structures of modified TSX double-chain models were created using a tLEaP module and GLYCAM_06j-1 parameter set for carbohydrates embedded in the AMBER 14 program [38]. It should be noted that it is impossible to model infinite chains due to the limitation of computational time and resources. Therefore, all modified TSX models were generated from eight units of N and eight units of H, but all models showed different sequences of N and H monomer units. Moreover, each model has two chains with similar sequences of N and H monomer units. In the initial structure of each model, the distance between two TSX chains was 15 Å to avoid formations of the intermolecular interactions. The initial structures of only one TSX chain of four models are shown in Figure 2.

Model	Sequence	Molecular structure
1	NNHHNNHH	
2	NHNHNHNH	
3	NNHNHHNH	
4	NHNNHHNH	

Figure 2. Sequences and structures of the four modified TSX models.

Each modified double-chain TSX model was hydrated with approximately 50,000 TIP5P water molecules. A minimization step was performed, followed by 500 ps of NVT-MD simulation to heat it to 283 K. The temperature was controlled by the Langevin dynamics and the SHAKE algorithm was applied to constrain hydrogens. On the following stage, 1 ns of NPT-MD simulation was performed at 1 atm and

283 K to equilibrate the system. After that, 100 ns of NPT-MD simulation was carried out for data analysis. A 2 fs time step and a non-bonded cutoff of 10 Å with the periodic boundary condition based on the Particle Mesh Ewald method were applied throughout simulations. The coordinate root-mean-square deviation (RMSD) profile was computed from all atoms and compared with the minimized structure of each model. Graphs of RMSD (Å) versus simulation time (ns) were plotted (Figure 3). The RMSD profile of each model displayed that, in the last 30 ns of dynamics, its fluctuation was in a small range (~3 Å). This means that the MD simulation can give a stable trajectory in the last 30 ns of dynamics. Therefore, the intermolecular interaction and structural properties were analyzed in the last 30 ns of dynamics.

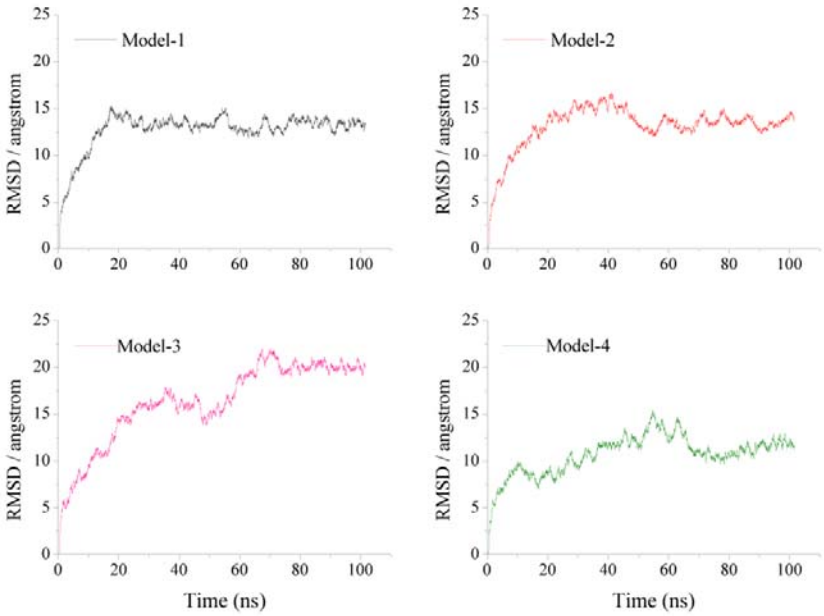

Figure 3. The RMSD profiles of model-1 to model-4.

The SAXS profile of each model was also calculated since it can be used to determine the shape of the oligomers and polymers in solution. In this study, a saxs_md module embedded in AMBER 14 was used to calculate the SAXS profile from the MD trajectory. The calculated SAXS profile was used to determine the radius of gyration (R_G) according to the Guinier approximation [39-44] given by:

$$I(q) \propto \exp\left(\frac{-R_G^2 q^2}{3}\right)$$

where q is the scattering vector and I(q) is the excessive intensity. I(q) is the difference of the scattering intensity between the sample and blank calculated by subtracting the average intensities over the time and the volume of the blank from the sample. It should be noted that the sample used in this study was the TSX model in aqueous solution, while the blank contained a volume of aqueous solution. In addition, the Guinier approximation for a rod-like structure was further applied to determine the cross-sectional radius of gyration (R_{Gc}) of the rod-like particle [39, 42-45]. The equation of R_{Gc} calculation is as follows;

$$q \cdot I(q) \approx \exp\left(\frac{-R_{Gc}^2 \cdot q^2}{2}\right)$$

3. RESULTS AND DISCUSSION

The electrostatic energy and van der Waals (vdW) energy profiles of each model calculated from heating, equilibration, and production steps are shown in Figure 4.

In each model, the electrostatic energy increased dramatically in a range of 0 ns to 5 ns of dynamics. After 71 ns of dynamics, the electrostatic energy of all models fluctuated around 11,400 kcal/mol. The electrostatic interactions of model-3 and model-2 were weaker than those of model-4 and model-1. For the vdW energy, during the duration of 0 ns to 40 ns of dynamics, it decreased continuously. After that, the fluctuation of the vdW energy of each model was quite different. The vdW interactions of model-3 and model-4 are weaker than that of model-2 and model-1. These results revealed that model-1 had the electrostatic and vdW interactions stronger than the other three models. It was reported that the modified TSX model is an uncharged molecule; hence the vdW interaction should be a prominent interaction for the molecular aggregations of TSX chains [25, 27, 34, 36-37]. Apart from the electrostatic energy, these results indicated that the vdW energy seems to play a crucial role in aggregations of the modified TSX model.

The Kratky plots used to determine the molecular shape [46] of all models are shown in Figure 5.

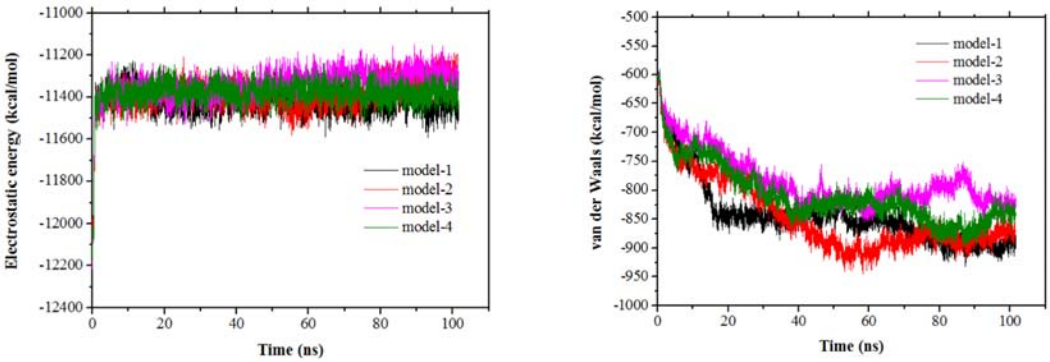

Figure 4. The profiles of electrostatic energy (left) and vdW energy (right) of model-1 to model-4.

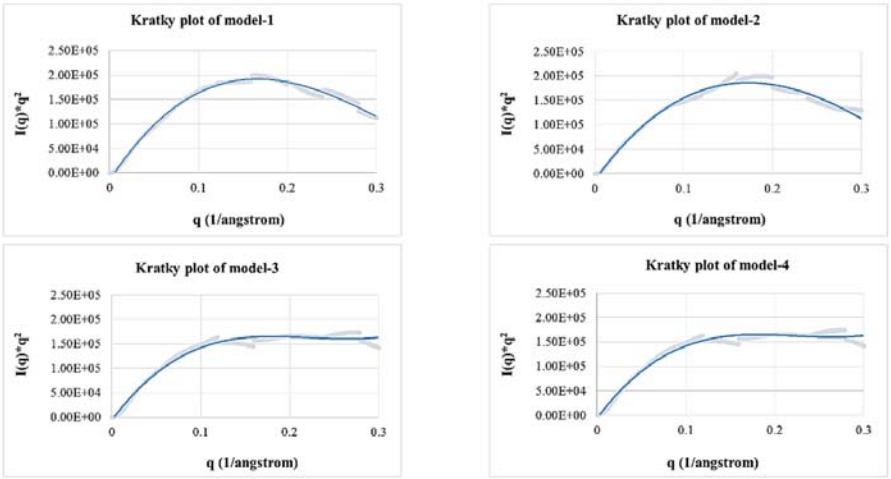

Figure 5. The Kratky plots of model-1 to model-4.

A trend solid line was plotted based on the simulated SAXS data (blue shaded points). These trend lines were similar to those of TSX reported in Ref. [10, 21]. The shape of the trend line of each model revealed that each modified TSX model had a rod-like structure. Besides, two modified TSX chains of model-1 and model-2 could aggregate more while the model-3 and model-4 had less gathering.

The Guinier plots of all models were carried out (data are not shown) and they were used to calculate the R_G and R_{Gc} values of each model (Table 1).

Table 1. The R_G, R_{Gc}, R_{End}, and SASA values of model-1 to model-4.

Name	R_G/Å	R_{Gc}/Å	R_{End}/Å	SASA/Å^2
model-1	41.8	5.0	142	14060
model-2	43.0	5.3	153	14078
model-3	42.7	5.6	134	15819
model-4	43.0	5.6	148	14739

The R_G values of all models were smaller than that of a native TSX polymer. This means that the modified TSX models were more packed than the native TSX polymer. Moreover, the R_{Gc} values of each single chain of TSX monomers and dimers were reported in a range of 3-4 Å [10]. The R_{Gc} values of gels of TSX polymer formed by adding gellator increased considerately, ranging from 6-9 Å [24] since many TSX chains could aggregate. In this study, the number of TSX chains was limited to 2 chains; thus, the R_{Gc} values could be compared with those of the TSX monomers and dimers. The R_{Gc} values of all modified models were larger than those of the native TSX single and double chains. This suggests that two modified TSX chains could have a side-by-side aggregation.

The average values of end-to-end distance (R_{End}) and solvent accessible surface area (SASA) of each model calculated in the last 30 ns of dynamics are also reported in Table 1. The R_{End} values of an initial structure of two TSX chains of all models were ~165 Å. The decrease of the R_{End} value indicated that there was shrinkage of the modified TSX chain caused by either the molecular associations or bending of the two modified TSX chains. Moreover, the model with a higher SASA value could have a large number of water molecules around the TSX chains. In the last 30 ns of dynamics, the R_{End} value of the model-3 was smaller than those of model-1, model-4, and model-2. For SASA, the model-3 had the highest value and the model-4 was the second highest while those of model-1 and model-2 were almost equal. These results indicated that the TSX chains of model-3 were the shortest, but could contact with water best. The TSX chains of model-2 were slightly shrinked, but it could associate better than the model-3. The length of TSX chains of model-4 and model-1 was comparable, but the TSX chains of model-4 seemed to contact water molecules better than the TSX chains of model-1.

To investigate the molecular structure of two modified TSX chains in aqueous solution of each model, the VMD program [47] was applied to visualize the model in the last 30 ns of dynamics. The average molecular structure of each model (averaged from 3,000 snapshots) was also carried out.

It was found that the molecular structure of two TSX chains of each model in the last 30 ns of dynamics changed very slightly. Also, the average structure of each model could be used as the representative structure in the last 30 ns of dynamics (Figure 6).

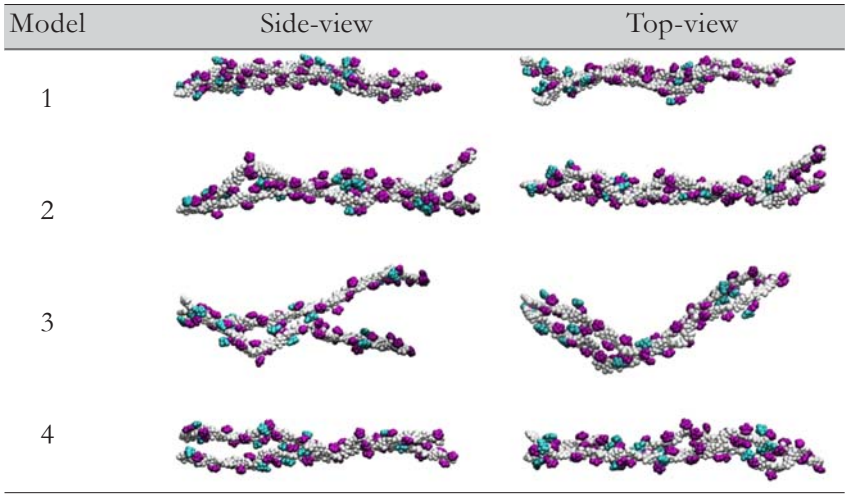

Figure 6. The average structure of two TSX chains of model-1 to model-4.

The molecular structures of all models showed local aggregations, but occurred at the different manners. All models displayed twisted and parallel-like structures except for model-3. These results were in accordance with the SAXS analysis. Compare with the other models, the two TSX chains of model-1 were the most highly packed with a worm-like and parallel-like structure. The Glu residues (white sphere) and Xyl residues (purple sphere) of a chain of model-1 could interact with those residues of another chain while the Gal residues (green sphere) exposed to water molecules. The TSX structure of model-2 was linear-like, but it had less associations than model-1 because there were two gaps between the chains and their chain ends separated from each other. The structure of model-3 was significantly bent and had the least aggregation. The TSX structure of model-4 was twisted and linear-like. For the model-3 and model-4, a half of each modified TSX chain separated from each other. Noticeably, at the region of TSX chain separation or in big gaps between two chains, Gal residues formed moderately strong intermolecular hydrogen bonds to Gal or Xyl or Glu residues. This was consistent with prior studies that the Gal residue was a hydrophilic part that could hinder the intermolecular interactions of TSX glucan main chains [24, 26-27]. Also, the reduction of Gal could promote the gelation due to the reduction of steric hindrance between TSX chains [24, 26-27]. From the MD results of this study, we found that the model-1 could be the most highly dense and had a worm-like structure because most of the Gal residues exposed themselves to bind with water molecules and the Glu and Xyl residues were more hydrophobic, interacting via the non-bonded interactions. These results revealed that the position of removed Gal was quite important for gelation of TSX since it could promote aggregation as could be seen in the model-1.

4. CONCLUSION

Four models of 50% galactose removal of two TSX chains in aqueous solution, in this study, were designed from eight N and H monomer units. Each model had different positions of the N and H monomer units to observe the role of the sequences of each modified TSX model in terms of aggregation. Each model was simulated in the same conditions using AMBER 14 for 100 ns of dynamics. After the MD simulation was performed at 283 K, the system could reach the equilibrium after 70 ns of dynamics and the analysis was performed in the last 30 ns of dynamics. The MD results revealed that the non-bonded interactions, especially the vdW interaction, played a crucial role in the aggregation of all modified TSX models. The vdW interaction showed more negative values when two TSX chains associated well. The Kratky plot suggested that model-1 had more aggregation and had a worm-like and parallel-like structure. Moreover, this study revealed that the Gal residue could hinder the TSX aggregation since it is more hydrophilic. The Glu and Xyl residues are more hydrophobic; hence, their intermolecular interactions could promote the TSX aggregations in aqueous solution. The aggregations of two modified TSX chains of model-1 to model-4 also implied that the sequences of eight N and H monomer units could have a significant role in the molecular aggregation of the TSX chains. In addition, the MD results indicated that model-1 could be the most possible model representing a possible structure of a TSX hydrogel.

ACKNOWLEDGEMENTS

This research was financially supported via grant numbers WU58201 and WU59603 from Walailak University, Thailand. The authors would like to thank the Theoretical and Computational Modeling (TCM) Research Unit, School of Science, Walailak University and the Structural and Computational Biology Research Group, Department of Biochemistry, Faculty of Science, Chulalongkorn University for all computational supports.

REFERENCES

[1] Suisha F., Kawasaki N., Miyazaki S., Shirakawa M., Yamatoya K., Sasaki M. and Attwood D., *Int. J. Pharmaceut.*, 1998; **172(1-2)**: 27-32.

[2] Kawasaki N., Ohkura R., Miyazaki S., Uno Y., Sugimoto S. and Attwood D., *Int. J. Pharmaceut.*, 1999; **181(2)**: 227-234.

[3] Miyazaki S., Kawasaki N., Kubo W., Endo K. and Attwood D., *Int. J. Pharmaceut.*, 2001; **220(1-2)**: 161-168.

[4] Hoffman A.S., *Adv. Drug Deliv. Rev.*, 2002; **54(1)**: 3-12.

[5] Takahashi A., Suzuki S., Kawasaki N., Kubo W., Miyazaki S., Loebenberg R., Bachynsky J. and Attwood D., *Int. J. Pharmaceut.*, 2002; **246(1-2)**: 179-186.

[6] Hoare T.R. and Kohane D.S., *Polymer*, 2008; **49(8)**: 1993-2007.

[7] Chen D., Guo P., Chen S., Cao Y., Ji W., Lei X., Liu L., Zhao P., Wang R., Qi C., Liu Y. and He H., *Mater. Med.*, 2012; **23(4)**: 955-62.

[8] Heimbach J.T., Egawa H., Marone P.A., Bauter M.R. and Kennepohl E., *Int. J. Toxicol.*, 2013; **32(3)**: 198-208.

[9] Mahajan H.S., Tyagi V.K., Patil R.R. and Dusunge S.B., *Carbohydr. Polym.*, 2013; **91(2)**: 618-25.

[10] Urakawa H., Mimura M. and Kajiwara K., *Trends Glycosci. Glycotechnol.*, 2002; **14(80)**: 355-376.

[11] Setty C.M., Deshmukh A.S. and Badiger A.M., *Int. J. Biol. Macromol.*, 2014; **67**: 28-36.

[12] Freitas R., Martin S., Santos G., Valenga F., Buckeridge M., Reicher F. and Sierakowski M., *Carbohydr. Polym.*, 2005; **60(4)**: 507-514.

[13] Sims I.M., Gane A.M., Dunstan D., Allan G.C., Boger D.V., Melton L.D. and Bacic A., *Carbohydr. Polym.*, 1998; **37(1)**: 61-69.

[14] Hoffman M., Jia Z., Pena M.J., Cash M., Harper A. and Blackburn A.R., *Carbohydr. Res.*, 2005; **340(11)**: 1826-1840.

[15] Vaaje-Kolstad G., Farkas V., Fincher G.B. and Hrmova M., *Arch. Biochem. Biophys.*, 2010; **496(1)**: 61-68.

[16] Zhang Q., Brumer H., Agren H. and Tu Y., *Carbohydr. Res.*, 2011; **346(16)**: 2595-2602.

[17] Busato A.P., Reicher F., Domingues R. and Silveira J.L.M., *Mater. Sci. Eng.: C*, 2009; **29(2)**: 410-414.

[18] Yamanaka S., Mimura M., Urakawa H., Kajiwara K., Shirakawa M. and Yamatoya K., *Sen'i Gakkaishi*, 1999; **55(12)**: 590-596.

[19] Ogawa K., Hayashi T. and Okamura K., *Int. J. Biol. Macromol.*, 1990; **12(3)**: 218-222.

[20] Umemura M. and Yuguchi Y., *Carbohydr. Res.*, 2005; **340(16)**: 2520-2532.

[21] Hirun N., Rugmai S. and Sangfai T., *Int. J. Biol. Macromol.*, 2012; **51(4)**: 423-430.

[22] Taylor I.E.P. and Atkins E.D.T., *FEBS Lett.*, 1985; **181(2)**: 300-302.

[23] Koziol A., Cybulska J., Pieczywek P.M. and Zdunek A., *Food Biophys.*, 2015; **10(4)**: 396-402.

[24] Picout D.R., Ross-Murphy S.B., Errington N. and Harding S.E., *Biomacromolecules*, 2003; **4(3)**: 799-807.

[25] Muller F., Manet S., Jean B., Chambat G., Boue F., Heux L. and Cousin F., *Biomacromolecules*, 2011; **12(9)**: 3330-3336.

[26] York W.S., van Halbeek H., Darvill A.G. and Albersheim P., *Carbohydr. Res.*, 1990; **200(0)**: 9-31.

[27] Shirakawa M., Yamatoya K. and Nishinari K., *Food Hydrocoll.*, 1998; **12(1)**: 25-28.

[28] Mishra A. and Malhotra A.V., *J. Mater. Chem.*, 2009; **19(45)**: 8528-8536.

[29] Klouda L. and Mikos A.G., *Eur. J. Pharmaceut. Biopharmaceut.*, 2008; **68(1)**: 34-45.

[30] Hirun N., Tantishaiyakul V., Sangfai T., Rugmai S. and Soontaranon S., *Polym. Bull.*, 2016; **73(8)**: 2211-2226.

[31] Jo T.A., Petri D.F.S., Beltramini L.M., Lucyszyn N. and Sierakowski M.R., *Carbohydrate Polymers*, 2010; **82(2)**: 355-362.

[32] Mkedder I., Travelet C., Durand-Terrasson A., Halila S., Dubreuil F. and Borsali R., *Carbohydr. Polym.*, 2013; **94(2)**: 934-9.

[33] Muller F., Jean B., Perrin P., Heux L., Boue F. and Cousin F., *Macromol. Chem. Phys.*, 2013; **214(20)**: 2312-2323.

[34] Yamanaka S., Yuguchi Y., Urakawa H., Kajiwara K., Shirakawa M. and Yamatoya K., *Sen'i Gakkaishi*, 1999; **55(11)**: 528-532.

[35] Ruel-Gariepy E. and Leroux J.C., *Eur. J. Pharmaceut. Biopharmaceut.*, 2004; **58(2)**: 409-26.

[36] Brun-Graeppi A.K.A.S., Richard C., Bessodes M., Scherman D., Narita T., Ducouret G. and Merten O.W., *Carbohydr. Polym.*, 2010; **80(2)**: 555-562.

[37] Nisbet D.R., Crompton K.E., Hamilton S.D., Shirakawa S., Prankerd R.J., Finkelstein D.I., Horne M.K. and Forsythe J.S., *Biophys. Chem.*, 2006; **121(1)**: 14-20.

[38] Case D.A., Babin V., Berryman J.T., Betz R.M., Cai Q., Cerutti D.S., Cheatham T.E., Darden T.A., Duke R.E., Gohlke H., Goetz A.W., Gusarov S., Homeyer N., Janowski P., Kaus J., Kolossvary I., Kovalenko A., Lee T.S., LeGrand S., Luchko T., Luo R., Madej B., Merz K.M., Paesani F., Roe D.R., Roitberg A., Sagui C., Salomon-Ferrer R., Seabra G., Simmerling C.L., Smith W., Swails J., Walker R.C., Wang J., Wolf R.M., Wu X. and Kollman P.A., AMBER 14, 14; University of California: San Francisco, 2014.

[39] Glatter O. and Kratky O., *Small Angle X-ray Scattering*, Academic Press: 1982.

[40] Suzuki S., Yukiyama T., Ishikawa A., Yuguchi Y., Funane K. and Kitamura S., *Carbohydr. Polym.*, 2014; **99(Supplement C)**: 432-437.

[41] Webber V., de Carvalho S.M. and Barreto P.L.M., *Carbohydr. Polym.*, 2012; **90(4)**: 1744-1749.

[42] Boyard N., Vayer M., Sinturel C., Seifert S. and Erre R., *Eur. Polym.J.*, 2005; **41(6)**: 1333-1341.

[43] Janicki J., *J. Alloys Compd.*, 2004; **382(1-2)**: 61-67.

[44] Slusarczyk C., *J. Alloys Compd.*, 2004; **382(1-2)**: 68-74.

[45] Yuguchi Y., Thu Thuy T.T., Urakawa H. and Kajiwara K., *Food Hydrocoll.*, 2002; **16(6)**: 515-522.

[46] Yuguchi Y., Tran V.T., Bui L.M., Takebe S., Suzuki S., Nakajima N., Kitamura S. and Thanh T.T., *Carbohydr. Polym.*, 2016; **147**: 69-78.

[47] Humphrey W., Dalke A. and Schulten K., *J. Mol. Graph.*, 1996; **14(1)**: 33-38.